Enhancement of 1.5 μm emission under 980 nm resonant excitation in Er and Yb co-doped GaN epilayers

Q. W. Wang, J. Li, J. Y. Lin, and H. X. Jiang[a)]
Department of Electrical and Computer Engineering, Texas Tech University, Lubbock, Texas 79409, USA

(Received 13 September 2016; accepted 3 October 2016; published online 12 October 2016)

The Erbium (Er) doped GaN is a promising gain medium for optical amplifiers and solid-state high energy lasers due to its high thermal conductivity, wide bandgap, mechanical hardness, and ability to emit in the highly useful 1.5 μm window. Finding the mechanisms to enhance the optical absorption efficiency at a resonant pump wavelength and emission efficiency at 1.5 μm is highly desirable. We report here the *in-situ* synthesis of the Er and Yb co-doped GaN epilayers (Er + Yb:GaN) by metal-organic chemical vapor deposition (MOCVD). It was observed that the 1.5 μm emission intensity of the Er doped GaN (Er:GaN) under 980 nm resonant pump can be boosted by a factor of 7 by co-doping the sample with Yb. The temperature dependent PL emission at 1.5 μm in the Er + Yb:GaN epilayers under an above bandgap excitation revealed a small thermal quenching of 12% from 10 to 300 K. From these results, it can be inferred that the process of energy transfer from Yb^{3+} to Er^{3+} ions is highly efficient, and non-radiative recombination channels are limited in the Er + Yb:GaN epilayers synthesized *in-situ* by MOCVD. Our results point to an effective way to improve the emission efficiency of the Er doped GaN for optical amplification and lasing applications. *Published by AIP Publishing*. [http://dx.doi.org/10.1063/1.4964843]

Rare earth (RE) doped semiconductors have been extensively investigated for applications in optoelectronics and optical communications. It is well established that the thermal stability of RE emission increases with an increase in the energy gap and the *ionicity* of the host materials.[1–4] As such, GaN has been recognized as an excellent host for RE doping.[4–7] In particular, the erbium (Er) doped GaN (Er:GaN) has been extensively studied.[8–14] Er:GaN is a very promising gain material for optical amplifiers[15] and high energy lasers[16] due to its emission at the wavelength of 1.5 μm, which coincides with the wavelength of lowest attenuation in silica optical fibers,[17–19] and it has high transmission in the atmosphere,[20] and has a relatively high upper limit of eye-safe laser exposure.[21] Moreover, GaN possesses a high thermal conductivity ($\kappa = 253$ W/m·K) and a low thermal expansion coefficient ($\alpha \approx 3.53 \times 10^{-6}$ °C^{-1}),[22] making it highly attractive as a laser gain medium because the maximum achievable lasing power for a solid-state laser, to the first order, is characterized by the thermal shock parameter of κ/α^2.[23–26] For all the emerging applications, finding mechanisms to further enhance the Er emission at 1.5 μm in Er:GaN is highly desirable.

It has been well established that Er and ytterbium (Yb) co-doping in a solid host is an effective approach to enhance the Er emission at 1.5 μm under 980 nm resonant excitation.[24,27–31] This is due to the fact that the absorption cross section of Yb^{3+} at 980 nm is about one order of magnitude larger than that of Er^{3+}. In the Er and Yb co-doped materials, Yb^{3+} ions act as sensitizers by absorbing 980 nm excitation photons and then transferring energy resonantly from their excited $^2F_{5/2}$ state to the $^4I_{11/2}$ level of Er^{3+} ions.[24,27–31] This efficient resonant energy transfer process is facilitated by the close match between the energy levels of the $^2F_{5/2}$ state of Yb^{3+} and the $^4I_{11/2}$ state of Er^{3+}. This transfer is then followed by a rapid nonradiative decay to the first $^4I_{13/2}$ excited manifold of Er^{3+} ions, after which a direct transition to the $^4I_{15/2}$ ground state of Er^{3+} occurs, resulting in the 1.5 μm emission.[31] The incorporation of Yb at a doping level similar to that of Er is thus expected to provide a nearly one order of magnitude enhancement in the effective optical absorption efficiency at 980 nm and hence a higher emission efficiency at 1.5 μm.[31] Different methods have been employed to obtain Er and Yb co-doped semiconductors so far, including magnetron sputtering[27,28] and ion-implantation.[29] Compared to these methods, *in-situ* co-doping of Er and Yb via epitaxial growth has the advantages of providing a more uniform distribution of RE concentrations and reduced impact to the crystalline quality of the host crystals;[30] however, this had not been previously attempted in GaN. We report here the *in-situ* synthesis of the Er and Yb co-doped GaN epilayers (Er + Yb:GaN) using metal-organic chemical vapor deposition (MOCVD).

The inset of Fig. 1 shows the schematic structure of the RE doped GaN epilayers (RE:GaN) used in this study, which were grown on the (0001) sapphire substrates. Trimethylgallium (TMG) and NH_3 served as the Ga and N sources, respectively. The precursors used for Yb and Er dopants were tris(cyclopentadienyl)ytterbium and tris(isopropylcyclopentadienyl)erbium, respectively. The precursors for Ga, Yb, and Er were held in stainless steel bubblers at 3 °C, 60 °C, and 60 °C, respectively, and were carried into the reactor by H_2 gas, and their flow rates were controlled by metal-sealed mass flow controllers. Prior to the growth of the RE doped epilayer, a thin GaN buffer layer was first deposited on the sapphire substrate at 550 °C, followed by the growth of an undoped GaN epilayer template of 1.2 μm in thickness. This was then followed by the growth of a 0.5 μm RE doped GaN epilayer. The growth temperature of the GaN epilayer template and RE doped GaN

a)hx.jiang@ttu.edu

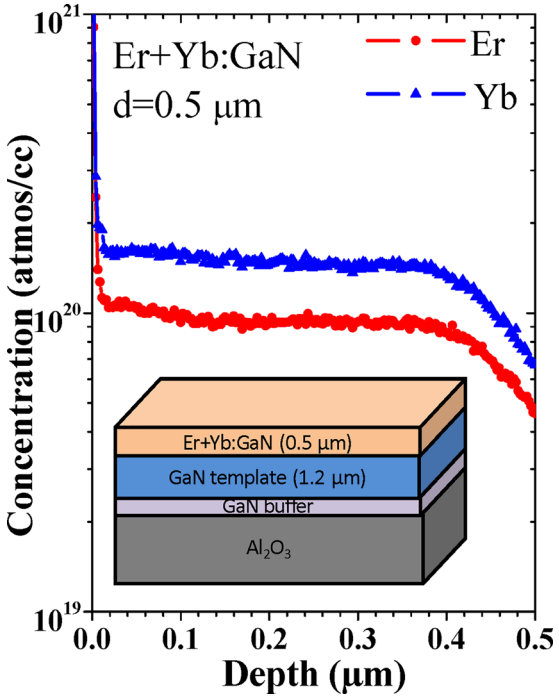

FIG. 1. SIMS profiles of Er and Yb concentrations in an Er + Yb:GaN epilayer grown under a Yb flow rate of 1.8 SLM and Er flow rate of 2.2 SLM. The inset is a schematic structure of Er + Yb:GaN epilayers used in this study.

epilayers was 1050 °C. During the growth process, an interferometer consisting of a 670 nm laser was used to monitor the growth rate and surface conditions, and the typical growth rate was 1.5 μm/h. The relative Er and Yb concentrations in the RE doped GaN epilayers were controlled by the flow rates of hydrogen to the bubblers containing the metal organic sources of Er and Yb. Consequently, the reported flow rates of Er and Yb are referring to the flow rates of hydrogen to the bubblers of Er and Yb, respectively. For comparison studies, pure Yb doped GaN (Yb:GaN) and Er doped GaN (Er:GaN) epilayers were also synthesized to serve as reference samples to guide the growth of the Er + Yb:GaN epilayers. The Er + Yb:GaN epilayers were grown using similar growth conditions established for the Er:GaN and Yb:GaN epilayers. Secondary-ion mass spectrometry (SIMS) was performed by Evans Analytical Group (EAG, Inc.) to probe the Er and Yb concentration profiles in the RE doped GaN epilayers. For instance, for an Er + Yb:GaN epilayer grown under a Yb flow rate of 1.8 standard liters per minute (SLM) and an Er flow rate of 2.2 SLM, SIMS results shown in Fig. 1 revealed that the concentrations of Er and Yb are quite uniform throughout the crystal and are about 1.0×10^{20} and 1.5×10^{20} atoms/cm^3, respectively. The effects of co-doping on the 1.5 μm emission properties of the Er + Yb:GaN epilayers were probed by photoluminescence (PL) spectroscopy. For room temperature PL spectra measurements, the excitation sources used consist of diode lasers operating at 375 nm and 980 nm, and the infrared PL spectra near 1.5 μm were recorded by an InGaAs infrared photodetector in conjunction with a spectrometer providing a spectral resolution of 3 nm. The temperature dependent PL spectra near 1.5 μm were excited by a frequency-tripled Ti:Sapphire laser at 260 nm and recorded by a 1.3-m monochromator providing a spectral resolution of 0.1 nm. The impact of Er and Yb co-doping on the crystalline quality of Er + Yb:GaN epilayers was evaluated by X-ray diffraction (XRD) measurements.

To provide a reference for the co-doped samples and verify the incorporation of Yb, the room temperature PL emission spectra of Yb:GaN epilayers grown under varying Yb flow rates were measured under a near bandgap excitation ($\lambda_{exc} = 375$ nm), and the results are shown in Fig. 2(a). The Yb:GaN epilayers exhibit emission peaks around 1 μm, resulting from the quasi-three-level $^2F_{5/2} \rightarrow {}^2F_{7/2}$ transition in Yb^{3+} ions.[31] These emission lines have been previously observed in the Yb ion-implanted materials[29,32] and the Yb doped InP.[30] The integrated emission intensity near 1 μm of Yb:GaN epilayers as a function of the Yb flow rate shown in Fig. 2(b) confirms that the Yb^{3+} related emission intensity increases almost linearly with an increase in the Yb flow rate employed during the growth, establishing appropriate flow rates for Yb.

To obtain the Er + Yb:GaN epilayers, the Er flow rate was set at a value of 2.2 SLM, and the Yb flow rate was varied from 0.9 to 2.4 SLM with an increment of 0.3 SLM. XRD was used to characterize the influence of Yb incorporation on the crystalline quality of the Er + Yb:GaN epilayers. A pure Er doped GaN epilayer (Er:GaN) grown at an Er flow rate of 2.2 SLM has a typical full width at half maximum (FWHM) of the GaN (0002) XRD rocking curve (ω-scan) of ~430 arcsec. As shown in Fig. 3(a), the FWHM of GaN (002) rocking curve increases with an increase in the Yb flow rate (or Yb concentration) for the Er + Yb co-doped epilayers. For a clear illustration, we plot in Fig. 3(b) the FWHM of GaN (002) rocking curve as a function of the Yb flow rate, and the results indicate that FWHM increases roughly linearly with the Yb flow rate

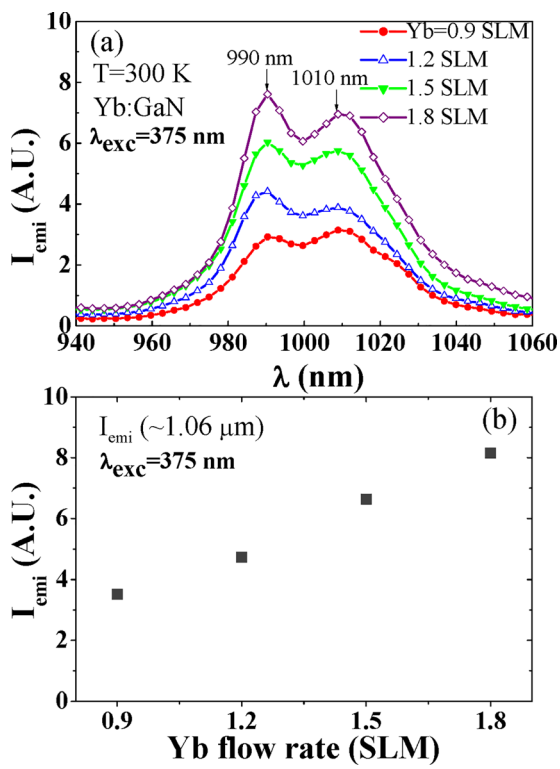

FIG. 2. (a) Room temperature PL spectra of Yb:GaN obtained under a near band edge excitation ($\lambda_{exc} = 375$ nm). (b) Integrated PL intensity near 1 μm (integrated from 940 to 1060 nm) as a function of the Yb flow rate.

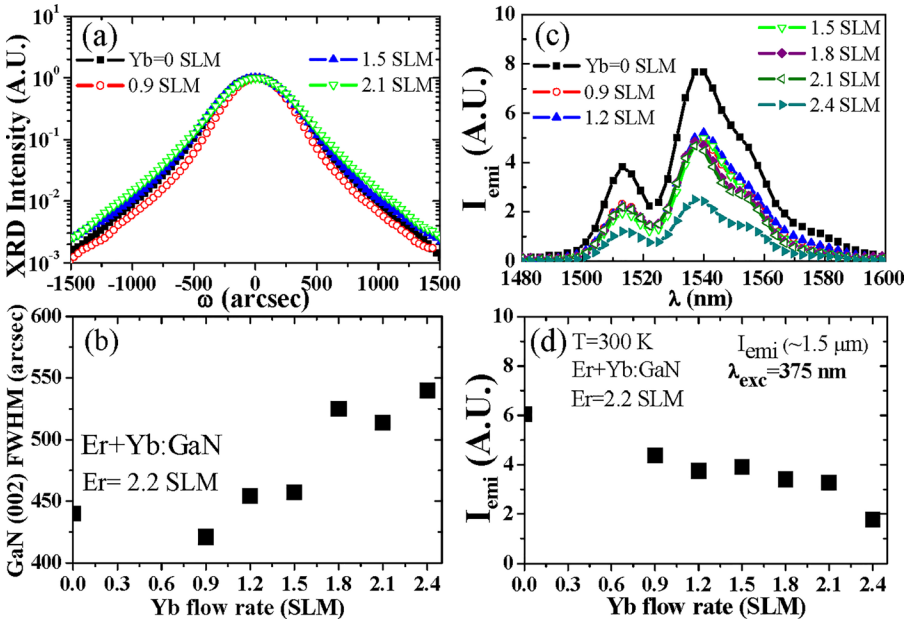

FIG. 3. (a) The XRD rocking curves of GaN (002) of the representative Er + Yb:GaN epilayers grown under varying Yb flow rates, whereas the Er flow rate was fixed at 2.2 SLM. (b) Plot of the full width at half maximum (FWHM) of the GaN (002) XRD rocking curve as a function of the Yb flow rate from 0 to 2.4 standard liters per minute (SLM), whereas the Er flow rate was fixed at 2.2 SLM. (c) Room temperature PL spectra of the same set Er + Yb:GaN epilayers grown under varying Yb flow rates under a near band edge excitation ($\lambda_{exc} = 375$ nm). (d) Integrated PL intensity near 1.5 μm (integrated from 1.48 to 1.6 μm) as a function of the Yb flow rate under a near band edge excitation ($\lambda_{exc} = 375$ nm).

and reaches ~540 arcsec for a Yb flow rate of 2.4 SLM. The results shown in Fig. 3(b) thus suggest that increasing the Yb concentration introduces more defects in the Er + Yb co-doped GaN epilayers during growth. This can be attributed to the fact that both the atomic sizes of Er and Yb ions are larger than that of Ga. During *in-situ* doping via MOCVD growth, Er and Yb are expected to replace Ga,[33,34] and their incorporation will induce stress in GaN due to the difference in the atomic sizes between Yb/Er atoms and Ga atoms. Therefore, a certain number of defects and dislocations will be generated in order to compensate for the atomic size differences as well as stress in the Er + Yb:GaN epilayers.

The PL emission spectra near 1.5 μm of the same set of Er + Yb:GaN epilayers have also been measured at room temperature under a near band edge excitation ($\lambda_{exc} = 375$ nm), and the results are shown in Fig. 3(c). The integrated emission intensity as a function of the Yb flow rate is plotted in Fig. 3(d). The results clearly show that the emission intensity near 1.5 μm under a near band edge excitation ($\lambda_{exc} = 375$ nm) decreases with an increase in the Yb flow rate, corroborating the observation of a reduction of crystalline quality with an increase in the Yb flow rate shown in Figs. 3(a) and 3(b). In a band-to-band or near band edge excitation scheme, the excitation of RE ions has to involve the generation of free or bound excitons and their subsequent energy transfer to RE ions. The results shown in Figs. 3(c) and 3(d) suggest that the generation efficiency of excitons as well as their energy transfer to Er^{3+} ions under a near bandgap excitation scheme is impacted by an increase in the dislocation density or reduction in the crystalline quality, which in turn reduced the 1.5 μm emission intensity. It was previously observed that the optical attenuation coefficient at 1.5 μm in Er:GaN waveguides increases linearly with the GaN (002) XRD rocking curve linewidth.[35] The present results of XRD and 1.5 μm PL emission under a band edge excitation hint that a tradeoff between the benefits gained from co-doping and impact of co-doping on the crystalline quality may need to be considered for the implementation of practical devices such as Er:GaN waveguide optical amplifiers.

The expected major benefit of Yb and Er co-doping is the enhancement of the absorption efficiency at 980 nm via the sensitization effect.[24,27–31] The room temperature PL spectra of the same set of Er + Yb:GaN epilayers grown under varying Yb flow rates from 0 to 2.4 SLM and a fixed Er flow rate of 2.2 SLM were measured under 980 nm resonant excitation, and the results are presented in Fig. 4(a). For the Yb flow rates below 1.0 SLM, there is no gain in the Er related emission intensity at 1.5 μm in Er + Yb:GaN over Er:GaN. The improvement in the 1.5 μm emission intensity in the Er + Yb:GaN epilayers over Er:GaN epilayers becomes gradually visible when the Yb flow rate is increased beyond 1.0 SLM. The integrated emission intensity near 1.5 μm is plotted in Fig. 4(b) as a function of the Yb flow rate. It is clear that the Er related emission intensity at 1.5 μm reaches a maximum enhancement factor of 7 when the Yb flow rate was at 1.8 SLM, *beyond* which a *further increase* in the Yb rate resulted in a reduction in the emission intensity at 1.5 μm. This behavior could be related to a reduction in the crystalline quality or Yb ion-ion cluster formation at higher Yb flow rates. However, the observed enhancement in the 1.5 μm emission efficiency in MOCVD grown Er + Yb:GaN epilayers over Er:GaN epilayers is consistent with the expected sensitization effect.[24,27–31]

A low thermal quenching of 20% in the 1.54 μm emission from 10 to 300 K has been previously observed in the Er:GaN epilayers for an above bandgap excitation ($\lambda_{exc} = 263$ nm).[12] A band-to-band excitation can excite both the isolated RE centers as well as defect-related RE optical centers.[36] In the case of isolated RE optical centers, the photo-generated excitons are trapped immediately by Er^{3+} ions affected *very little* by any *non–radiative* processes. In the case of defect-related optical centers (RE ions strongly associated with nearby defects or impurities), the photo-generated excitons are first trapped by impurities or local defects near RE ions, followed by a non-radiative energy transfer to RE ions. Therefore, a band-to-band excitation process could involve more non-radiative recombination channels than a resonant excitation at 980 nm, which provides a photon energy perfectly matching with a

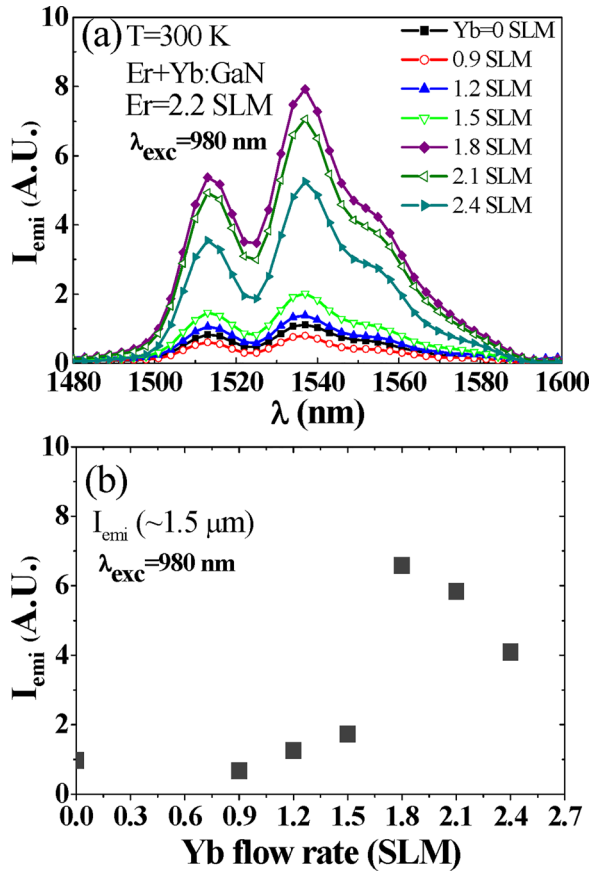

FIG. 4. (a) Room temperature PL spectra of Er + Yb:GaN epilayers under 980 nm resonant excitation. (b) Integrated PL intensity near 1.5 μm (integrated from 1.48 to 1.6 μm) as a function of the Yb flow rate under 980 nm resonant excitation ($\lambda_{exc} = 980$ nm).

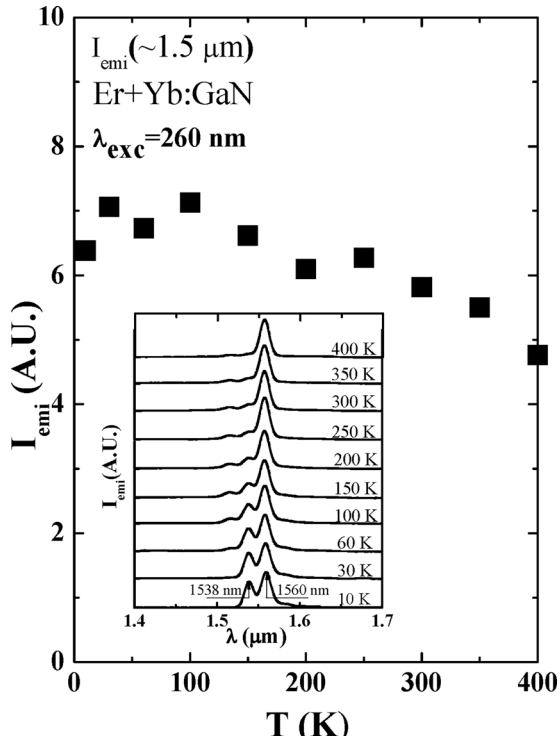

FIG. 5. Integrated PL emission intensity near 1.5 μm (integrated from 1.48 to 1.6 μm) of an Er + Yb:GaN epilayer (grown at a Yb flow rate of 1.8 SLM and Er flow rate of 2.2 SLM) as a function of temperature obtained from the temperature dependent PL spectra shown in the inset.

higher-lying inner shell transition in both Yb^{3+} and Er^{3+} ions. To make a fair direct comparison with the Er:GaN epilayers, the temperature dependent PL spectra of the co-doped sample exhibiting the maximum enhancement in the 1.5 μm emission, i.e., an Er + Yb:GaN epilayer grown at a Yb flow rate of 1.8 SLM and Er flow rate of 2.2 SLM, were measured under an above bandgap excitation using $\lambda_{exc} = 260$ nm and recorded by a 1.3-m monochromator, as shown in the inset of Fig. 5. Two emission peaks at 1.538 μm and 1.560 μm were resolved more prominently in the low temperature PL spectra. The integrated PL emission intensity near 1.5 μm as a function of temperature for this sample is plotted in Fig. 5. The results revealed a thermal quenching of 12% in the 1.5 μm emission intensity from 10 K to 300 K. The small thermal quenching associated with the 1.5 μm emission resulting from the 1st excited manifold ($^4I_{13/2}$) to the ground state ($^4I_{15/2}$) in Er^{3+} ions implies that the process of energy transfer from the Yb^{3+} to Er^{3+} is very efficient and is also much shorter than the recombination lifetime of the $^2F_{5/2}$-$^2F_{7/2}$ transition in Yb^{3+} ions.[29] Furthermore, this small thermal quenching implies that there are many more isolated RE optical centers than the defect-related optical centers in the Er+Yb:GaN epilayers as in the case of Er:GaN epilayers, in which more than 70% of the contribution to the 1.5 μm emission is from the isolated Er optical centers.[36]

In summary, the Er and Yb co-doped GaN epilayers have been synthesized *in-situ* by MOCVD. The XRD and PL results revealed that co-doping boosts the 1.5 μm emission efficiency by a factor of up to 7 under 980 nm excitation despite a reduced crystalline quality due to the incorporation of Yb. A small thermal quenching of only 12% of the 1.5 μm emission from 10 K to 300 K was measured for the Er + Yb:GaN epilayers, implying that the energy transfer processes are very efficient and the non-radiative recombination channels are limited. The results suggest that the Er + Yb:GaN epilayers are promising for devices applications at room and elevated temperatures.

The work was supported by High Energy Laser Joint Technology Office (W911NF-12-1-0330) and was monitored by Dr. Mike Gerhold of ARO. The authors would like to thank Xiaozhang Du for help with the temperature dependence of the PL measurements. Jiang and Lin would also like to acknowledge the support of Whitacre Endowed Chairs by the AT & T Foundation.

[1]P. N. Favennec, H. L'Halidon, M. Salvi, D. Moutonnet, and Y. Le Guillou, Electron. Lett. **25**, 718 (1989).
[2]R. Birkhahn, M. Garter, and A. J. Steckl, Appl. Phys. Lett. **74**, 2161 (1999).
[3]A. J. Neuhalfen and B. W. Wessels, Appl. Phys. Lett. **60**, 2657 (1992).
[4]J. M. Zavada and D. Zhang, Solid-State Electron. **38**, 1285 (1995).
[5]M. Pan and A. J. Steckl, Appl. Phys. Lett. **83**, 9 (2003).
[6]A. J. Steckl, M. J. Garter, D. S. Lee, J. Heikenfeld, and R. H. Birkhahn, Appl. Phys. Lett. **75**, 2184 (1999).
[7]T. Arai, D. Timmerman, R. Wakamatsu, D. Lee, A. Koizumi, and Y. Fujiwara, J. Lumin. **158**, 70 (2015).
[8]R. G. Wilson, R. N. Schwartz, C. R. Abernathy, S. J. Pearton, N. Newman, M. Rubin, T. Fu, and J. M. Zavada, Appl. Phys. Lett. **65**, 992 (1994).
[9]S. Kim, S. J. Rhee, X. Li, J. J. Coleman, S. G. Bishop, and P. B. Klein, Appl. Phys. Lett. **76**, 2403 (2000).

[10]D. M. Hansen, R. Zhang, N. R. Perkins, S. Safvi, L. Zhang, K. L. Bray, and T. F. Kuech, Appl. Phys. Lett. **72**, 1244 (1998).
[11]X. Wu, U. Hommerich, J. D. MacKenzie, C. R. Abernathy, S. J. Pearton, R. Schwartz, R. G. Wilson, and J. M. Zavada, Appl. Phys. Lett. **70**, 2126 (1997).
[12]C. Ugolini, N. Nepal, J. Y. Lin, H. X. Jiang, and J. M. Zavada, Appl. Phys. Lett. **89**, 151903 (2006).
[13]R. Dahal, C. Ugolini, J. Y. Lin, H. X. Jiang, and J. M. Zavada, Appl. Phys. Lett. **97**, 141109 (2010).
[14]A. Braud, *Excitation Mechanisms of RE Ions in Semiconductors, Topics in Applied Physics: Rare Earth Doped III-Nitrides for Optoelectronic and Spintronic Applications* Vol. 124, edited by K. O'Donnell and V. Dierolf (Springer, The Netherlands, 2010), pp. 269–308.
[15]R. Dahal, C. Ugolini, J. Y. Lin, H. X. Jiang, and J. M. Zavada, Appl. Phys. Lett. **95**, 111109 (2009).
[16]Z. Y. Sun, J. Li, W. P. Zhao, J. Y. Lin, and H. X. Jiang, Appl. Phys. Lett. **109**, 052101 (2016).
[17]R. J. Mears, L. Reekie, I. M. Jauncey, and D. N. Payne, Electron. Lett. **23**, 1026 (1987).
[18]E. Desurvire, J. Simpson, and P. C. Becker, Opt. Lett. **12**, 888 (1987).
[19]J. D. B. Bradley and M. Pollnau, Laser Photonics Rev. **5**, 368–403 (2011).
[20]R. W. Fenn, J. D. Mill, S. A. Clough, L. S. Rothman, W. O. Gallery, E. P. Shettle, R. E. Good, F. E. Volz, and F. X. Kneizys, "Optical and infrared properties of the atmosphere," in *Handbook of Geophysics and the Space Environment*, edited by A. S. Jursa (Air Force Geophysics Laboratory, Hanscom AFB, MA, 1985),
[21]J. A. Zuclich, D. J. Lund, and B. E. Stuck, Health Phys. **92**, 15 (2007).
[22]H. Shibata, Y. Waseda, H. Ohta, K. Kiyomi, K. Shimoyama, K. Fujito, H. Nagaoka, Y. Kagamitani, R. Simura, and T. Fukuda, Mater. Trans. **48**, 2782 (2007).
[23]W. Koechner, *Solid-State Laser Engineering*, 5th ed. (Spring-Verlag, Berlin, Heidelberg, 1999).
[24]G. Huber, C. Krankel, and K. Petermann, "Solid-state lasers: Status and future," J. Opt. Soc. Am. **27**, B93 (2010).
[25]J. Vetrovec, "Solid-state high-energy laser," Proc. SPIE **4632**, 104 (2002).
[26]A. Giesen and J. Speiser, IEEE J. Sel. Top. Quantum Electron. **13**, 598 (2007).
[27]V. Prajzler, Z. Burian, I. Hüttel, J. Špirková, J. Hamáček, J. Oswald, J. Zavadil, and V. Peřina, Acta Polytech. **46**, 49 (2006).
[28]I. B. Gallo, A. Braud, and A. R. Zanatta, Opt. Express **21**, 28394 (2013).
[29]C. Strohhöfer and A. Polman, Opt. Mater. **21**, 705 (2003).
[30]K. Uwai, H. Nakagome, and K. Takahei, Appl. Phys. Lett. **50**, 977 (1987).
[31]C. Grivas, Prog. Quantum Electron. **45–46**, 3 (2016).
[32]W. M. Jadwisienczak, J. Wang, H. Tanaka, J. Wu, R. Palai, H. Huhtinen, and A. Anders, J. Rare Earth **28**, 931 (2010).
[33]K. C. Mishra, V. Eyert, and P. C. Schmidt, Z. Phys. Chem. **221**, 1663 (2007).
[34]U. Wahl, E. Alves, K. Lorenz, J. G. Correia, T. Monteiro, B. De Vries, A. Vantomme, and R. Vianden, Mater. Sci. Eng., B **105**, 132 (2003).
[35]I. W. Feng, W. P. Zhao, J. Li, J. Y. Lin, H. X. Jiang, and J. Zavada, Appl. Opt. **52**, 5426 (2013).
[36]D. K. George, M. D. Hawkins, M. McLaren, H. X. Jiang, J. Y. Lin, J. M. Zavada, and N. Q. Vinh, Appl. Phys. Lett. **107**, 171105 (2015).